Journal of COMPUTATIONAL CHEMISTRY

Quantum Monte Carlo Study of the Retinal Minimal Model $C_5H_6NH_2^+$

Emanuele Coccia and Leonardo Guidoni*

In this work, we study the electronic and geometrical properties of the ground state of the Retinal Minimal Model $C_5H_6NH_2^+$ using the variational Monte Carlo (VMC) method by means of the Jastrow antisymmetrized geminal power (JAGP) wavefunction. A full optimization of all wavefunction parameters, including coefficients, and exponents of the atomic basis, has been achieved, giving converged geometries with a compact and correlated wavefunction. The relaxed geometries of the cis and trans isomers present a pronounced bond length alternation pattern characterized by a C=C central double bond slightly shorter than that reported by the CASPT2 structures. The comparison between different basis sets indicates converged values of geometrical parameters, energy differences, and dipole moments even when the smallest wavefunction is used. The compactness of the wavefunction as well as the scalability of VMC optimization algorithms on massively parallel computers opens the way to perform full structural optimizations of conjugated biomolecules of hundreds of electrons by correlated methods like Quantum Monte Carlo. © 2012 Wiley Periodicals, Inc.

DOI: 10.1002/jcc.23071

Introduction

Rhodopsin is a well-known light-detecting protein belonging to the family of G-protein-coupled receptors and responsible for the dim light vision of vertebrates.[1–7] The Retinal chromophore (retinal protonated schiff base, RPSB), bound to the seven-helix transmembrane protein by a protonated Schiff base,[4] upon photon absorption induces a cis/trans isomerization from 11-cis to all-trans isomer which in turn generates structural changes in the protein, activating the signal cascade leading to vision.[4,8] Such cis/trans isomerization represents one of the faster (~200 fs) and efficient (quantum yield of ~0.65) chemical processes in nature,[4,7,9] and the role of the protein environment is fundamental, since the same reaction in solution is much slower.[7,10] QM/MM dynamics calculations and experimental data coming from ultrafast femtosecond spectroscopy give evidence that the isomerization path involves a S_1/S_0 conical intersection (CI), with the reaction coordinate being mainly dominated by the torsional angle around the central double bond.[7]

Plenty of literature from both experimental and theoretical investigations, has been produced over the last 15 years on gas phase retinal models and on Rhodopsin, focusing the attention on several issues, such as the determination of the gas phase energies and geometries in the ground and excited states,[10–19] the features of the isomerization mechanism,[7,9,10,20] the effect of the protein environment on the geometrical and electronic properties and the corresponding energy shifts in the visible absorption spectra.[8,16,21–29]

Several works have been devoted to the study of small Retinal models to capture the essential properties of the full system (e.g., the isomerization mechanism) on smaller molecules.[10,20,30–40] To correctly address the ground and excited state geometries and energies of these molecules in their ground or excited states the use of correlated methods such as CASPT2, MP2, and QMC is required,[10,33] due to the conjugated nature of the polyenic chain.

The retinal Minimal Model $C_5H_6NH_2^+$ (Fig. 1), composed of three conjugated double bonds, has been extensively studied by the quantum chemistry community since it is supposed to have an isomerization path qualitatively similar to that of the Retinal.[10,30] Geometry optimizations (GEOs) for the ground state show a good agreement among CASPT2, MP2, variational Monte Carlo (VMC), and DFT/B3LYP approaches, giving a pronounced bond length alternation (BLA), while the CASSCF result is characterized by a sensitively stronger BLA.[10] Appreciable differences instead are seen for the optimized structure of the Minimal Model S_1 state, for which CASSCF exhibits two minima (one with inversion of the BLA pattern, the second with a general lengthening of the bonds preserving the BLA value),[10,33] whereas CC2, VMC, CASPT2 and CCSD approaches find only one minimum, with a preserved or reduced "ground state-like" BLA.[10]

The CASSCF S_1 minimum energy path (MEP) of $C_5H_6NH_2^+$ starts with a bond stretching which leads, in turn, to the region of the PES in which the S_1/S_0 CI occurs, with the C1—C2=C3—C4 angle close to 90°.[30] CASSCF dynamics simulations show evidence of a sub-picosecond isomerisation with a high quantum yield,[41] with the central C2=C3 bond involved in the torsion, mimicking what happens in the biological environment with the full chromophore[30]; the $S_1 \rightarrow S_0$ decay is barrierless and this fact could explain the very fast

E. Coccia, L. Guidoni
Dipartimento di Scienze Fisiche e Chimiche, Universitá degli Studi dell'Aquila, via Vetoio (Coppito) 67100, L'Aquila, Italy
E-mail: leonardo.guidoni@univaq.it

Contract/grant sponsor: European Research Council ("MultiscaleChemBio" within the VII Framework Program of the European Union); Contract/grant number: 240624.

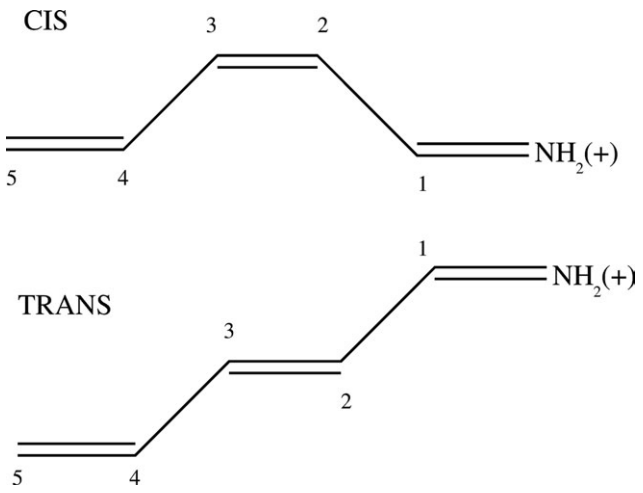

Figure 1. Cis and trans isomers of the Retinal Minimal Model.

isomerization of the chromophore and the high quantum yield in the protein environment.

Olivucci and coworkers also presented a detailed CASPT2//CASSCF and TDDFT//CASSCF investigation of the isomerization path of the Minimal Model,[35] to validate the TDDFT MEP on the excited state.

Full GEOs of the complete RPSB chromophore (120 valence electrons) were reported using CASSCF and MP2 calculations,[11,14] whereas, at the best of our knowledge, no CASPT2 and CC data are yet available. The inclusion of a larger treatment of the quantum region within a QM/MM scheme, such as the RPSB counterion (Glu 113) and surrounding residues would be probably important to investigate the effects of the protein on the Retinal BLA and on the excitation energies and represent a further challenge for correlated methods.

An alternative to traditional multideterminant wavefunction methods is represented by Quantum Monte Carlo techniques. In particular, VMC methods, which are based on the stochastic calculation of the expectation value of the full electronic Hamiltonian on a given trial wavefunction, have been recently used to successfully perform gas phase GEO of molecular systems.[10,42,43] The variational ansatz in VMC is given by highly correlated many-body wavefunctions characterized by different functional forms and by a set of variational parameters usually optimized through an energy minimization procedure.[44] Dynamical electronic correlation is described by applying the Jastrow factor,[45] a symmetric positive-defined term depending explicitly on the electron–nucleus and electron–electron distances. Projection methods, such as diffusion Monte Carlo and lattice regularized diffusion Monte Carlo are also able to go beyond the variational guess, accessing to the exact ground-state energy of the system, within the fixed-node approximation.[46–49]

The quality of QMC methods is comparable to that obtained by standard correlated quantum chemistry methods (or even higher), as verified by several applications concerning different areas of physics and chemistry: materials,[47,50–52] hydrogen bonding and Van der Waals systems,[53,54] electronic excitations in gas phase,[10,43,55,56] molecular polarizabilities and biochemistry.[19,57,58] From the computational point of view QMC methods can be considered a promising correlated quantum chemistry tool for the study of large molecules, thanks to two technical reasons: the excellent scalability of the algorithms up to tens of thousands of processors on recent high performance computing facilities; and the favorable scaling of the computational time with the system size ($N^{3/4}$, with N the number of electrons).[46–48,59]

In this work, we carry out full wavefunction and structural VMC optimizations of the cis and trans isomers of the Retinal Minimal Model, calculating isomerization energies and ground state dipole moments. The convergence of these results with respect to the size of the basis sets will be also analyzed with the aim to select a compact wavefunction that can be easily used for larger systems. An extensive comparison with the data coming from other high level calculations will be also shown to point out how our computational scheme can provide accurate energies and relaxed structures, with a special focus on the BLA, that is a key geometrical parameter for conjugated chromophores. At the same time, we will provide benchmarks on larger systems, supporting the feasibility of performing accurate structural optimizations of conjugated biomolecules of hundreds electrons at the VMC level.

In the "Methods" section the VMC method is briefly reviewed together with the trial wavefunction definition and the strategy applied for the GEO; details of the wavefunctions used in the present work are also shown. Our results on the ground state of the Retinal Minimal Model are reported in "Results and Discussion" focusing the attention on the structural parameters and on the convergence of the properties of interest as a function of the wavefunction complexity. Conclusions and perspectives are found in the last section underlining the concrete possibility of QMC to become a reference tool in the electronic structure calculations of large correlated molecular systems of biological relevance.

Methods

VMC

The VMC energy E_{VMC} is defined as the minimum of the expectation value of the electronic Hamiltonian $\hat{H}$ over the variational parameters $\alpha = \{\alpha_i\}$ of a trial wavefunction Ψ_T, given a specific nuclear configuration $\mathbf{R}$[44,46]:

$$E_{VMC} = \min_{\alpha} E[\Psi_T(\mathbf{x};\alpha,\mathbf{R})], \tag{1}$$

where

$$E[\Psi_T] = \frac{\int \Psi_T(\mathbf{x};\alpha,\mathbf{R})\hat{H}\Psi_T(\mathbf{x};\alpha,\mathbf{R})d\mathbf{x}}{\int \Psi_T^2(\mathbf{x};\alpha,\mathbf{R})d\mathbf{x}} \tag{2}$$

assuming Ψ_T to be real. In VMC the latter integral over the electronic coordinate $\mathbf{x}$ ($\mathbf{r}$ and σ) is written in terms of the local energy $E_L(\mathbf{x};\alpha,\mathbf{R}) = \hat{H}\Psi_T(\mathbf{x};\alpha,\mathbf{R})/\Psi_T(\mathbf{x};\alpha,\mathbf{R})$, and of a probability density $\Pi(\mathbf{x};\alpha,\mathbf{R}) = \frac{\Psi_T^2(\mathbf{x};\alpha,\mathbf{R})}{\int \Psi_T^2(\mathbf{x};\alpha,\mathbf{R})d\mathbf{x}}$

$$E[\Psi_T] = \int \Pi(\mathbf{x};\alpha,\mathbf{R})E_L(\mathbf{x};\alpha,\mathbf{R})d\mathbf{x} = \langle \hat{H} \rangle_{\Pi} \tag{3}$$

The value of the integral in Eq. (3) is then estimated as a sum over a set of points in the configurational space of the electronic Cartesian and spin coordinates **x**, generated stochastically by a Metropolis algorithm according to the probability density $\Pi(\mathbf{x};\alpha,\mathbf{R})$[60]; brackets indicate the average on Π. The Ψ_T optimization procedure is based on the linear method described in Ref. [54].

VMC GEO

The structural optimization within the VMC scheme implies the simultaneous minimization of the energy functional with respect to the variational parameters α of Ψ_T and the nuclear coordinates **R**:

$$E_{\mathrm{VMC}}^{\mathrm{OPT}} = \min_{\alpha,\mathbf{R}} E[\mathbf{R};\Psi_T(\mathbf{x};\alpha,\mathbf{R})]. \tag{4}$$

A standard steepest descent method is employed for the minimum searching. The optimization requires the evaluation of the ionic forces acting along all the coordinates **R**, defined for each nucleus *A* as:

$$\mathbf{F}_A(\mathbf{R}) = -\nabla_{\mathbf{R}_A} E_{\mathrm{VMC}}(\mathbf{R};\alpha(\mathbf{R})), \tag{5}$$

where $\alpha(\mathbf{R})$ implicitly depends on **R** because the minimum energy condition [Eq. (1)] has to be satisfied at fixed **R**. VMC forces for the nucleus A are given by the following expression[46]:

$$\begin{aligned}\mathbf{F}_A(\mathbf{R}) = &-\left\langle \frac{dE_L}{d\mathbf{R}_A}\right\rangle_\Pi + 2\left\{\langle E_L\rangle_\Pi \left\langle \frac{d\ln[\Psi_T]}{d\mathbf{R}_A}\right\rangle_\Pi \right.\\ &\left. -\left\langle E_L \frac{d\ln[\Psi_T]}{d\mathbf{R}_A}\right\rangle_\Pi\right\} = \mathbf{F}_A^{H-F}(\mathbf{R}) + \mathbf{F}_A^{P}(\mathbf{R}),\end{aligned} \tag{6}$$

that are respectively the Hellmann–Feynman $\mathbf{F}_A^{H-F}(\mathbf{R}) = -\left\langle \frac{dE_L}{d\mathbf{R}_A}\right\rangle_\Pi$ and Pulay $\mathbf{F}_A^{P}(\mathbf{R}) = 2\left\{\langle E_L\rangle_\Pi \left\langle \frac{d\ln[\Psi_T]}{d\mathbf{R}_A}\right\rangle_\Pi - \left\langle E_L \frac{d\ln[\Psi_T]}{d\mathbf{R}_A}\right\rangle_\Pi\right\}$ terms. The Pulay term is zero in the case of an exact eigenstate in the limit of complete basis sets and when Ψ_T is expanded into an originless basis set like plane waves.

Further improvement to reduce the variance on the calculated forces is achieved using the so-called space warp coordinate transformation (SWCT).[10,43,61–64] At nodal surface the unbound variance of the forces has been removed using the reweighting method.[43,65] In addition, we used the Adjoint Algorithmic Differentiation scheme to obtain analytical derivatives of the complex function resulting by the combined use of pseudopotential and SWCT.[43] The overall computational overload for calculating forces is only a factor 4 with respect to the single energy evaluation, independently on the system-size. More details on the calculation of forces can be found in Refs. [43] and [64].

Jastrow antisymmetrized geminal power wavefunction

Sorella and coworkers[42,43,58,66–68] have recently introduced the Jastrow Antisymmetrised Geminal Power (JAGP) trial wavefunction, based on Pauling's resonating valence bond representation. The JAGP is defined as the product between an antisymmetric geminal power (AGP) and a Jastrow factor $J(\mathbf{r})$ (we omit here the parametric dependence on α and **R** of Ψ_T)

$$\Psi_T(\mathbf{x}) = \Psi_{\mathrm{AGP}}(\mathbf{x}) \times J(\mathbf{r}) \tag{7}$$

and includes both static and dynamical electronic correlation[53,54,69,70]; **r** represents the 3 *N* electron Cartesian coordinate, *J* is spin-independent to avoid spin contamination.[42,68]

For unpolarized molecular systems of *N* electrons and *M* nuclei, that is, $N/2 = N^{\uparrow} = N^{\downarrow}$, the AGP is written as

$$\Psi_{\mathrm{AGP}}(\mathbf{x}) = \hat{A}\prod_i^{N/2} \Phi_G\left(\mathbf{x}_i^{\uparrow};\mathbf{x}_i^{\downarrow}\right) \tag{8}$$

where $\hat{A}$ is the antisymmetrization operator and Φ_G is the Geminal pairing function:

$$\Phi_G(\mathbf{x}_i;\mathbf{x}_j) = \phi_G(\mathbf{r}_i,\mathbf{r}_j)\frac{1}{\sqrt{2}}\left(|\uparrow\rangle_i|\downarrow\rangle_j - |\uparrow\rangle_j|\downarrow\rangle_i\right). \tag{9}$$

The spatial function $\phi_G(\mathbf{r}_i,\mathbf{r}_j)$ is a linear combination of products of atomic orbitals:

$$\phi_G(\mathbf{r}_i,\mathbf{r}_j) = \sum_{A,B}^{M}\sum_{\mu,\nu} \lambda_{\mu_A\nu_B}\psi_{\mu_A}(\mathbf{r}_i)\psi_{\nu_B}(\mathbf{r}_j) \tag{10}$$

where the indexes μ and ν refer to the basis sets centered on the *A*th and *B*th nuclei.

The Jastrow term *J* is split into a product of several terms $J = J_1J_2J_{3/4}$, introducing dynamical correlation and satisfying the electron–electron and electron–nucleus cusp conditions.[43,58,71,72] The three/four body Jastrow $J_{3/4}$ includes the electron–electron-nuclei correlation

$$J_{3/4}(\mathbf{r}) = \exp\left\{\sum_{i<j}^{N}\varpi(\mathbf{r}_i,\mathbf{r}_j)\right\}, \tag{11}$$

where

$$\varpi(\mathbf{r}_i,\mathbf{r}_j) = \sum_{A,B}^{M}\sum_{\mu_A\nu_B} g_{\mu_A\nu_B}\chi_{\mu_A}(\mathbf{r}_i)\chi_{\nu_B}(\mathbf{r}_j). \tag{12}$$

Terms with $A = B$ represent the three body term, whereas terms with $A \neq B$ are four body terms, that describe the dynamical correlation of electrons on different atomic centers; in this work we have not used the J_4 term.

The JAGP compactness, combined with the use of efficient algorithms for the optimization of all parameters, including linear coefficients and exponents of the atomic basis sets,[54,73,74] leads to a fast convergence of the variational results for electronic and geometrical properties with the size of the basis sets.[43,75]

Computational details

Four different AGP wavefunctions have been defined for our study, named VMC1, VMC2, VMC3, and VMC4; the corresponding basis sets, together which the total number of variational parameters N_p^{AGP} are collected in Table 1. The starting parameters for the contraction of VMC1 and VMC2 are taken from the cc-pVDZ basis set, VMC3, and VMC4 are instead from aug-cc-pVDZ. As we employ scalar-relativistic energy-conserving pseudopotentials for C and N atoms in the calculations,[76,77] the

Table 1. AGP and J basis sets used in the present work.

AGP	Carbon	Nitrogen	Hydrogen	N_p^{AGP}
VMC1	(4s4p)/[2s2p]	(4s4p)/[2s2p]	(3s1p)/[2s1p]	4076
VMC2	(4s4p1d)/[2s2p1d]	(4s4p1d)/[2s2p1d]	(3s1p)/[2s1p]	7193
VMC3	(6s5p2d)/[3s3p2d]	(6s5p2d)/[3s3p2d]	(5s2p)/[3s2p]	21,178
VMC4	(4s2s*3p2p*2d*)/[3s3p2d]	(4s2s*3p2p*2d*)/[3s3p2d]	(3s2s*2p*)/[3s2p]	21,178
J_3	Carbon	Nitrogen	Hydrogen	N_p^J
	(3s2p)/[2s1p]	(3s2p)/[2s1p]	(2s1p)/[1s1p]	2160

N_p^{AGP} and N_p^J are the total number of parameters for the AGP and Jastrow term, respectively. The * corresponds to a STO (see text for details).

inner s orbital has been removed in all AGPs for such atoms. VMC1 and VMC2 differ in the presence of d orbitals; the dimension of the AGP matrix, coupling the single-electron atomic orbitals centered on different nuclei, almost doubles when moving from VMC1 to VMC2. VMC3 and VMC4 are clearly characterized by a larger variational space since polarization and diffuse functions are added; they get the same number N_p^{AGP} of optimizable parameters, the main difference arising from the use in VMC4 of a hybrid GTO/STO basis set.[58,78,79] Primitive Gaussian functions with exponents $\zeta_G > 15$ (30 for the augmented basis sets) are neglected because of the use of pseudopotentials, also resulting in a stable and efficient optimization procedure.[58]

The use of Slater functions for the uncontracted terms significantly improves the long range behaviour of Ψ_T, in terms of variational energy and convergence of properties like the dipole polarizability of molecular systems[58,79]; the initial exponents for the exponential functions are derived from the Gaussians through the simple relation $\zeta_S = \sqrt{2\zeta_G}$, where ζ_S is the exponent of the Slater function. All the variational parameters characterizing the wavefunction are fully optimized following the scheme described in Ref. [58] by releasing of the linear coefficients and the exponents of the atomic basis sets.[54] A contraction of Gaussian primitives of s and p type (Table 1) has been chosen for the three-body Jastrow term.

Each structural optimization point is composed of 2.7×10^6 QMC steps, each step including N proposed single electron moves. Calculations have been carried out on the JUGENE BlueGene/P (BG/P) cluster in Jülich (Germany). Scalability tests for the VMC GEO on BG/P show an almost perfect scaling (90% efficiency) up to 65536 CPU cores.

The average BLA is defined as the difference between the average value of the two single bonds and the average value of the three double bonds (also including the nitrogen):

$$\mathrm{BLA} = \frac{\mathrm{R(C1-C2)} + \mathrm{R(C3-C4)}}{2} - \frac{\mathrm{R(C1=N)} + \mathrm{R(C2=C3)} + \mathrm{R(C4=C5)}}{3}. \quad (13)$$

Dipole moments are calculated in the reference frame of the nuclear center of charge:

$$\mathbf{CC} = \frac{\sum_A Z_A \mathbf{R}_A}{\sum_A Z_A}, \quad (14)$$

where the index A runs over the nuclei and Z_A is the effective charge on the A-th nucleus.

Results and Discussion

Geometrical ground state features play a crucial role in tuning the excitation energies of the RPSB chromophore and its model systems, the effect being of the order of some tenths of eV.[10,16] Getting a reliable ground state geometry also represents a crucial step in the study of the isomerization pathways since an accurate Franck–Condon structure is fundamental as starting point for the path.

A key geometrical parameter regulating the ground and excited state properties in conjugated systems is the average BLA, defined in Eq. (13). The evaluation of such property is very sensitive to the used methodology, ranging in the case of the cis Retinal Minimal Model from a value of 0.065–0.112 Å, moving from DFT (PBE and BPW91) to CASSCF calculations.[34,35] The convergence of the average BLA and of all the bond distances using the VMC1 trial wavefunction during a GEO where all wavefunction parameters have been released, including linear coefficients and exponents of the atomic basis sets, is reported in Figure 2. To verify that our QMC

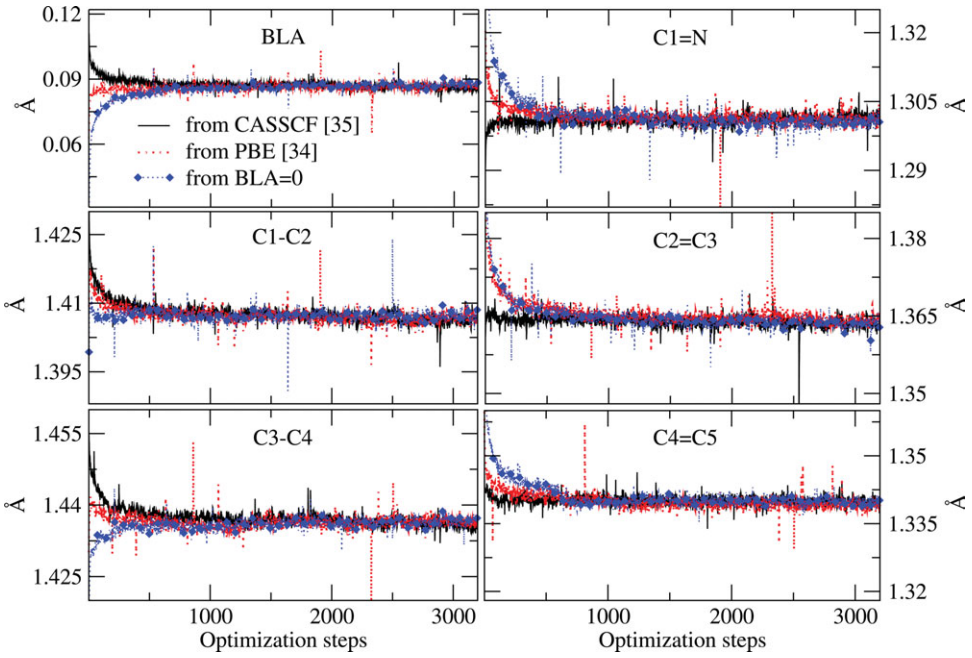

Figure 2. BLA and bond lengths evolution along the GEO path starting from different structures. VMC1 wavefunction has been used for the cis isomer.

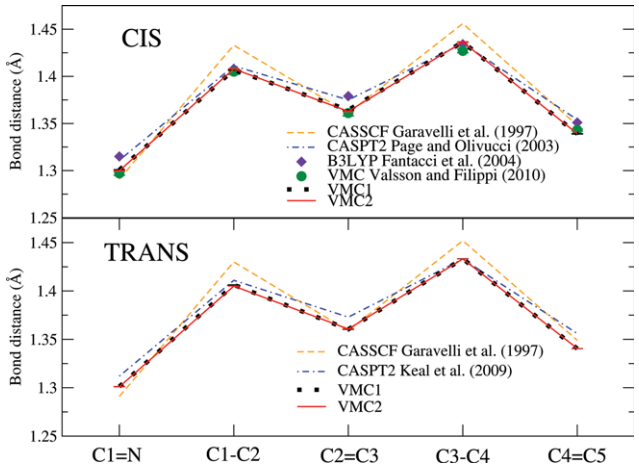

Figure 3. Upper panel: comparison of the BLA pattern calculated at VMC level with some literature data for the cis isomer. Lower panel: the same as above for the trans isomer. VMC1 and VMC2 refer to the Ψ_T definition explained in the text.

optimization procedure is robust with respect to the initial configuration, we have repeated the calculation starting from three structures with different BLA values: a large BLA (0.111 Å) from a CASSCF structure,[30] a small BLA (0.065 Å) from a DFT(PBE) one,[35] and a structure with no BLA. The data show that all simulations converge within 1000 optimization steps to the same geometry, demonstrating that no bias due to the initial configuration affects our procedure.

The VMC GEO has been applied to the cis and trans isomers using VMC1 and VMC2 wavefunctions (see Table 1 and Computational Details) enforcing the planarity of both systems.

The bond length pattern of the cis isomer is reported in the upper panel of Figure 3, compared with other available calculated data. VMC1 and VMC2 data are in perfect agreement indicating that the presence of d orbitals in the VMC2 basis set does not significantly influence the equilibrium bond length pattern. The two wavefunctions converge to very similar bond distances, leading to corresponding BLA values of 0.0869(1) Å and 0.0881(3) Å for VMC1 and VMC2 geometries, respectively. Our results are in agreement within about 0.001–0.009 Å in terms of bond lengths with previous VMC data reported by Valsson and Filippi.[10] The small differences can be probably attributed to the choice of the functional form of the trial wavefunction, a linear combination of spin-adapted configuration state functions multiplied by a Jastrow factor instead of JAGP.[10] VMC geometries are between the CASSCF and CASPT2 relaxed configurations,[10,30,33,34] reducing the exaggerated difference between single and double bonds seen in CASSCF but shortening the double bonds with respect to the CASPT2 description. An attenuated BLA with respect to the CASSCF results is found,[30,34] but larger than DFT, CASPT2, and MP2 findings.[10,33,35,37]

A similar behavior is found for the trans isomer (lower panel of Fig. 3 and Table 2); also in this case our BLA assumes an intermediate value [0.0858(2) Å with VMC1 and 0.0850(1) Å with VMC2] between the CASSCF 0.108 Å (a global shortening of all bonds is seen) and the CASPT2 0.075 Å (on the contrary, VMC single and double bonds are longer).[30,37]

Table 3 collects the bond angles calculated on VMC1 and VMC2 optimized structures for the cis isomer, compared with some representative, high-quality data in literature.[10,30,33,35,37] We can observe clearly that the use of the more compact VMC1 Ψ_T implies no substantial effects on angles, the larger differences being only 0.3° and 0.2° for the C_2—C_1=N and C_3=C_2—C_1 with respect to VMC2 values.[10,30,33,35,37] Finally, it is interesting to note that VMC2 results are very close to MP2,[33] as already pointed out for the BLA. The trans isomer bond angles are also reported in Table 3; VMC1 and VMC2 structures are characterized by essentially the same bond angle values, emphasizing again the reliability of VMC1 as wavefunction for the geometrical optimization.

To further validate the quality of our VMC approach, we have performed single point calculations on several structures using the set of basis sets VMC1–VMC4 described in Computational Methods. First, we evaluate the energy of CASSCF geometries of the cis and trans isomers as well as on the proposed structure of the CI[30] between S_0 and S_1 states, with the central dihedral angle close to 90°. The resulting energy differences are reported in Table 4 and compared with CASSCF and CASPT2 data: the first row of Table 4 refers to the cis/trans isomerization energy, the second one to the energy difference between the trans isomer (the most stable configuration) and the relaxed CI geometry. The more complex VMC2, VMC3, and VMC4 wavefunctions show an excellent agreement with the cis/trans

Table 2. Optimized bond lengths for the ground state S_0 of the *cis* and *trans* minimal model.

	C1=N	C1—C2	C2=C3	C3—C4	C4=C5	BLA
CIS						
VMC1	1.3008(1)	1.4068(2)	1.3643(1)	1.4364(1)	1.3390(1)	0.0869(1)
VMC2	1.2999(1)	1.4079(1)	1.3629(2)	1.4364(2)	1.3392(1)	0.0881(3)
VMC[10]	1.297(2)	1.405(3)	1.361(3)	1.427(2)	1.343(1)	0.082(3)
CASSCF[30]	1.291	1.433	1.361	1.456	1.348	0.111
CASSCF[34]	1.288	1.431	1.358	1.454	1.346	0.112
CASPT2[33]	1.311	1.411	1.375	1.435	1.354	0.076
CASPT2[10]	1.312	1.422	1.381	1.446	1.362	0.082
MP2[33]	1.309	1.411	1.371	1.437	1.351	0.080
MP2[10]	1.311	1.421	1.379	1.444	1.359	0.083
B3LYP[35]	1.315	1.408	1.379	1.434	1.351	0.073
PBE0[35]	1.308	1.406	1.374	1.431	1.348	0.075
BPW91[35]	1.324	1.412	1.389	1.435	1.362	0.065
PBE[35]	1.323	1.411	1.388	1.434	1.361	0.065
TRANS						
VMC1	1.3012(1)	1.4063(2)	1.3604(3)	1.4333(1)	1.3404(1)	0.0858(2)
VMC2	1.3010(2)	1.4051(2)	1.3607(3)	1.4331(1)	1.3406(1)	0.0850(1)
CASSCF[30]	1.291	1.430	1.359	1.452	1.349	0.108
CASPT2[37]	1.312	1.411	1.373	1.433	1.356	0.075

All the quantities are in Å. BLA is defined as the difference between the average values of single and double bonds, including the nitrogen.

Table 3. Bond angles (°) for the *cis* and *trans* isomers. VMC1 and VMC2 correspond to the present work.

	C2—C1=N	C3=C2—C1	C4—C3=C2	C5=C4—C3
CIS				
VMC1	123.83(1)	122.60(1)	128.70(1)	119.86(1)
VMC2	123.54(1)	122.81(2)	128.75(1)	119.85(1)
VMC[10]	123.9(2)	123.5(2)	128.9(1)	120.3(1)
CASSCF[30]	123.0	123.6	128.6	121.4
CASPT2[33]	123.2	123.1	128.5	120.2
CASPT2[37]	123.1	122.9	128.5	120.1
MP2[33]	123.4	122.9	128.7	119.8
B3LYP[33]	124.0	123.8	128.9	120.5
TRANS				
VMC1	124.54(2)	119.34(1)	124.28(1)	120.88(1)
VMC2	124.50(2)	119.20(2)	124.25(1)	120.83(1)
CASSCF[30]	124.0	120.1	124.2	122.1
CASSCF[37]	124.0	120.0	124.2	122.1
CASPT2[37]	124.1	119.4	124.2	121.0

isomerization CASPT2 energy values; the smallest VMC1 basis slightly overestimates the cis/trans energy of about 0.6 kcal/mol with respect to VMC4 values. All CI/trans energies are found in the range between 54.34(9) kcal/mol (VMC2) and 55.50(8) kcal/mol (VMC4), very close to the CASPT2 value of 54.3 kcal/mol.[30]

Cis/trans isomerization energies are also reported for VMC optimized structures (third and fourth rows of Table 4); the two structures do not show any sensitive shift due to the (small) geometrical differences reported above, confirming *a posteriori* that VMC1 is a good and reliable Ψ_T for obtaining optimized structures with a reduced computational effort. Furthermore, VMC single energy evaluations on VMC geometries agree well with VMC energies calculated on CASSCF structures, with fluctuations of about 0.1–0.2 kcal/mol.

The molecular dipole moment μ is computed with respect to the atomic center of charge, defined in Eq. (14), on cis and trans structures (Table 5). On the CASSCF structures, the dipole moment for both isomers does not essentially change from VMC1 to VMC4. For what concerns VMC structures, VMC1 and VMC2 geometries give a clear stabilization to μ along the four wavefunctions, for both cis and trans isomers; the differences between the dipole moments calculated on the VMC and on the CASSCF geometries (0.2–0.4 D for cis and 0.3–0.6 D for trans, with the exclusion of VMC4 on VMC1 structure) is mainly due to the less conjugated pattern of the CASSCF geometry.

In summary, the choice of the VMC1 wavefunction to perform geometrical optimization leads to a structure practically coincident to that obtained with the larger VMC2 wavefunction. The same behavior is observed for the evaluation of the molecular dipole moment; the accuracy on the cis/trans isomerization energy is about 0.5 kcal/mol.

Table 5. Dipole moments in Debye for the ground state S_0.

μ	Geometry	VMC1	VMC2	VMC3	VMC4
TRANS	CASSCF	4.58(1)	4.88(1)	4.64(1)	4.78(1)
CIS	CASSCF[30]	4.33(1)	4.36(1)	4.16(1)	4.28(1)
TRANS	VMC1	4.21(1)	4.28(1)	4.33(1)	4.63(1)
CIS	VMC1	3.92(1)	3.97(1)	3.98(1)	3.93(1)
TRANS	VMC2	–	4.25(1)	4.33(1)	4.34(1)
CIS	VMC2	–	4.01(1)	3.94(1)	3.92(1)

Results for cis and trans isomers are in the reference frame of the nuclear center of charge. The first two rows show the VMC findings on CASSCF structures, the other rows are from VMC1 and VMC2 structures. The second column indicates the level of theory employed for relaxing the structures.

Having in mind to apply this VMC GEO scheme to larger molecular targets, such as the Retinal and its surrounding residues, we have carried out some tests on systems with increasing number N of electrons as indicated in Table 6. We report the total CPU core-hours time per point on BG/P architecture during wavefunction optimization (WF, third column) and GEO (fourth column) for the following systems: the ethyne molecule C_2H_2, the Retinal Minimal Model, the gas-phase RPSB and a system including RPSB surrounded by one water molecule and two glutamic acids sidechains (Glu113 and Glu118) as observed in the crystallographic structure of the Bovine Rhodopsin.[80] VMC1 wavefunction has been used for all the systems. A regression fit with the formula (CPU core hours/point) $= aN^p$ (a and p the fitting parameters) gives a power p for the scaling equal to 2.5 for Ψ_T and 2.2 for the structural optimization. Such small scaling factor is fundamental for tackling electronic structure calculations of molecules of biological relevance like RPSB. It is important to point out that this result simply refers to the algorithmic dependence on the system size; to obtain a size-independent error on the total energies and forces, an "extra" power N should be added, since the variances grow as N, thus obtaining a scaling of $N^{3.5}$ for the wavefunction and $N^{3.2}$ for the GEOs, in agreement with the expected scaling reported by Ref. [47].

With the same statistics/point used here for the Minimal Model (2.7×10^6 QMC steps per each optimization point), we therefore estimate that about 4 millions of CPU core-hours are needed for a system with $N = 120$ and about 10 millions of CPU core-hours for a system with $N = 182$ to perform 1000

Table 4. Isomerization energies in kcal/mol for the ground state S_0.

ΔE	Geometry	CASPT230	CASSCF 30	VMC1	VMC2	VMC3	VMC4
CIS/TRANS	CASSCF[30]	3.5	3.39	4.27(8)	3.52(8)	3.85(8)	3.68(7)
CI/TRANS	CASSCF[30]	54.3	59.6	55.28(9)	54.34(9)	54.71(7)	55.50(8)
CIS/TRANS	VMC1	–	–	4.09(8)	3.57(8)	3.70(7)	3.68(7)
CIS/TRANS	VMC2	–	–	–	3.80(8)	3.75(8)	3.66(7)

The first two rows show the VMC results on CASSCF structures for both cis/trans and CI/trans energies (see text for details); the second two rows are from VMC1 and VMC2 structures for the cis/trans isomerization only. The second column indicates the level of theory employed for relaxing the geometry.

Table 6. Computational time and scalability of VMC energy and geometry optimizations for molecular systems of increasing number of electrons *N*.

System	*N*	CPU core-hours/WF point (h)	CPU core-hours/ GEO point (h)
C_2H	10	2.8	8.6
$CHNH_2^+$	32	27.2	124.3
RPSB	120	631.6	4333.9
RPSB + H_2O + Glu113 + Glu181	182	1818.9	10,574.7

Third and fourth columns report the total CPU core-hours (= elapsed real time × number of cores, for parallel runs) per each wavefunction (WF) and geometry (GEO) optimization point. A random walk statistics of 2.7×10^6 Monte Carlo steps is employed for each case. Computational tests were performed on Jugene BG/P cluster in Jülich (Germany) using the VMC1 wave function.

structural optimization points. Such computational requirement is now affordable on High Performance facilities, and can be exploited by QMC methods thanks to their embarrassing parallelism.

Conclusions

In this work, we have presented a full VMC study of the ground state properties of both the cis and trans isomers of the Retinal Minimal Model $C_5H_6NH_2^+$, which is a prototype of the RPSB in Rhodopsin. Wavefunction and GEOs have been carried out by optimizing all variational parameters of the JAGP wavefunction, a compact and highly correlated variational ansatz.

The structural optimization carried out at VMC level results in an average BLA of 0.0881(3) Å for the cis isomer and 0.0850(1) Å for the trans one. VMC1 and VMC2 AGP wavefunctions have been used, to verify the quality of the smaller VMC1 wavefunction and its capability of capturing the correct geometrical features of the conjugated system. The average BLA from VMC1 and VMC2 geometries essentially converges to the same structural minimum. VMC1 and VMC2 differ for the set of d orbitals introduced for C and N atoms, coming from the cc-pvDZ contraction; even the small VMC1 Ψ_T is able to correctly recover the BLA of the cis and trans isomers together with the bond angles. The very small differences observed with the more accurate VMC2 have no sensitive effect on the isomerization energies and on the dipole moments, calculated with four different trial wavefunctions, VMC1 and VMC2 included.

Our VMC BLA is between the large CASSCF result and CASPT2 values and very similar to MP2 and other VMC calculations (based on a trial function defined as a linear combination of spin-adapted configuration state functions for the determinantal part), in line with the idea that the inclusion of correlation effects reduces the difference between single and double bonds. In terms of bond angles, our findings are very close to MP2 and other VMC calculations. Furthermore, properties calculated at VMC level on VMC1 and VMC2 structures agree well with values extracted from a CASSCF geometry; high accuracy is guaranteed by the use of fully correlated QMC and can be easily obtained by improving the quality (and the number of variational parameters) of the trial Ψ_T.

The results shown in this work allow us to be confident with the use of the VMC1 trial wavefunction for GEO; the computational effort can be sensitively reduced, opening the way to the study of the full Retinal chromophore and, in general, of molecules of biological interest (~200/300 electrons) with QMC techniques, exploiting the possibilities offered by new generation High Performance Computing facilities.

Acknowledgments

The authors thank Sandro Sorella for the support provided on the TurboRVB QMC code[67] and Andrea Zen and Matteo Barborini for useful comments on the manuscript. They acknowledge for computational resources the PRACE Tier-0 Project N^o PRA053, the CINECA computer center and the Caliban HPC center of the University of L'Aquila.

Keywords: bond length alternation · conjugated molecules · electronic correlation · rhodopsin

How to cite this article: E. Coccia, L. Guidoni, *J. Comput. Chem.* **2012**, *33,* 2332–2339. DOI: 10.1002/jcc.23071

[1] T. Yoshizawa, G. Wald, *Nature* **1963**, *197,* 1279.
[2] G. Wald, *Science* **1968**, *162,* 230.
[3] K. Palczewski, T. Kumasaka, T. Hori, C. A. Behnke, H. Motoshima, B. A. Fox, I. L. Trong, D. C. Teller, T. Okada, R. E. Stenkamp, M. Yamamoto, M. Miyano, *Science* **2000**, *289,* 739.
[4] K. Palczewski, *Annu. Rev. Biochem.* **2006**, *75,* 743.
[5] M. Wanko, M. Hoffmann, T. Frauenheim, M. Elstner, *J. Comput. Aided Mol. Des.* **2006**, *20,* 511.
[6] M. B. Nielsen, *Chem. Soc. Rev.* **2009**, *38,* 913.
[7] D. Polli, P. Altoé, O. Weingart, K. M. Spillane, C. Manzoni, D. Brida, G. Tomasello, G. Orlandi, P. Kukura, R. A. Mathies, M. Garavelli, G. Cerullo, *Nature* **2010**, *467,* 440.
[8] U. F. Röhrig, L. Guidoni, A. Laio, I. Frank, U. Rothlisberger, *J. Am. Chem. Soc.* **2004**, *126,* 15328.
[9] I. Schapiro, M. N. Ryazantsev, L. M. Frutos, N. Ferré, R. Lindh, M. Olivucci, *J. Am. Chem. Soc.* **2011**, *133,* 3354.
[10] O. Valsson, C. Filippi, *J. Chem. Theory Comput.* **2010**, *6,* 1275.
[11] A. Cembran, R. Gonzalez-Luque, P. A. M. Merchan, F. Bernardi, M. Olivucci, M. Garavelli, *J. Phys. Chem. A* **2005**, *109,* 6597.
[12] L. H. Andersen, I. B. Nielsen, M. B. Kristensen, M. O. A. El Ghazaly, S. Haacke, M. B. Nielsen, M. A. Petersen, *J. Am. Chem. Soc.* **2005**, *127,* 12347.
[13] I. B. Nielsen, L. Lammich, L. H. Andersen, *Phys. Rev. Lett.* **2006**, *96,* 18304.
[14] S. Sekharan, O. Weingart, V. Buss, *Biophys. J. Biophys. Lett.* **2006**, *91,* L07.
[15] R. Send, D. Sundholm, *J. Phys. Chem. A* **2007**, *111,* 27.
[16] K. Bravaya, A. Bochenkova, A. Granovsky, A. Nemukhin, *J. Am. Chem. Soc.* **2007**, *129,* 13035.
[17] R. R. Zaari, S. Y. Y. Wong, *Chem. Phys. Lett.* **2009**, *469,* 224.
[18] J. Rajput, D. B. Rahbek, L. H. Andersen, A. Hirshfeld, M. Sheves, P. Altoé, G. Orlandi, M. Garavelli, *Angew. Chem.* **2010**, *122,* 1834.
[19] O. Valsson, C. Filippi, *J. Chehm. Phys. Lett* **2012**, *3,* 908.
[20] I. Schapiro, O. Weingart, V. Buss, *J. Am. Chem. Soc.* **2009**, *131,* 16.
[21] N. Ferré, M. Olivucci, *J. Am. Chem. Soc.* **2003**, *125,* 6868.

[22] T. Andruniow, N. Ferré, M. Olivucci, *Proc. Nat. Acad. Sci. USA* **2004**, *101,* 17908.
[23] U. F. Röhrig, L. Guidoni, U. Rothlisberger, *ChemPhysChem* **2005**, *6,* 1836.
[24] F. Blomgren, S. Larsson, *J. Comput. Chem.* **2005**, *26,* 738.
[25] J. A. Gascon, E. M. Sproviero, V. S. Batista, *Acc. Chem. Res.* **2006**, *39,* 184.
[26] P. B. Coto, A. Strambi, N. Ferré, M. Olivucci, *Proc. Nat. Acad. Sci. USA* **2006**, *103,* 17154.
[27] L. M. Frutos, T. Andruniow, F. Santoro, N. Ferré, M. Olivucci, *Proc. Nat. Acad. Sci. USA* **2007**, *104,* 7764.
[28] A. Altun, S. Yokoyama, K. Morokuma, *J. Phys. Chem. B* **2008**, *112,* 6814.
[29] A. Altun, S. Yokoyama, K. Morokuma, *J. Phys. Chem. B* **2008**, *112,* 16883.
[30] M. Garavelli, P. Celani, F. Bernardi, M. A. Robb, M. Olivucci, *J. Am. Chem. Soc.* **1997**, *119,* 6891.
[31] R. Gonzalez-Luque, M. Garavelli, F. Bernardi, M. Merchan, M. Olivucci, *Proc. Nat. Acad. Sci. USA* **2000**, *97,* 9379.
[32] L. De Vico, C. S. Page, M. Garavelli, F. Bernardi, R. Basosi, M. Olivucci, *J. Am. Chem. Soc.* **2001**, *124,* 4124.
[33] C. S. Page, M. Olivucci, *J. Comput. Chem.* **2003**, *24,* 298.
[34] A. Migani, M. A. Robb, M. Olivucci, *J. Am. Chem. Soc.* **2003**, *125,* 2804.
[35] S. Fantacci, A. Migani, M. Olivucci, *J. Phys. Chem. A* **2004**, *108,* 1208.
[36] M. Wanko, M. Hoffmann, P. Strodel, A. Koslowski, W. Thiel, F. Neese, T. Frauenheim, M. Elstner, *J. Phys. Chem. A* **2005**, *109,* 3606.
[37] T. W. Keal, M. Wanko, W. Thiel, *Theor. Chem. Acc.* **2009**, *123,* 145.
[38] J. J. Szymczak, M. Barbatti, H. Lischka, *J. Phys. Chem. A.* **2009**, *113,* 11907.
[39] R. Send, D. Sundholm, M. O. Johansson, F. Pawlowski, *J. Chem. Theory Comput.* **2009**, *5,* 2401.
[40] A. Mosca Conte, L. Guidoni, R. D. Sole, O. Pulci, *Chem. Phys. Lett.* **2011**, *515,* 290.
[41] O. Weingart, A. Migani, M. Olivucci, M. A. Robb, V. Buss, P. Hunt, *J. Phys. Chem A* **2004**, *108,* 4685.
[42] M. Casula, C. Attaccalite, S. Sorella, *J. Chem. Phys.* **2004**, *121,* 7110.
[43] M. Barborini, S. Sorella, L. Guidoni, *J. Chem. Theory Comput.* **2012**, *8,* 1260.
[44] D. Bressanini, P. J. Reynolds, In Advances in Chemical Physics: Monte Carlo Methods in Chemical Physics, Vol. 105; pp. 37; New York: Wiley **1999**.
[45] R. Jastrow, *Physical Review* **1955**, *98,* 1479.
[46] B. L. Hammond, W. A. Lester, Jr., P. J. Reynolds, Monte Carlo Methods in Ab-Initio Quantum Chemistry; Singapore: World Scientific, **1994**.
[47] W. M. C. Foulkes, L. Mitas, R. J. Needs, G. Rajagopal, *Rev. Mod. Phys.* **2001**, *73,* 33.
[48] D. M. Towler, In Computational Methods for Large Systems; Wiley, **2011**.
[49] P. J. Reynolds, D. M. Ceperley, B. J. Alder, W. A. Lester, Jr., *J. Chem. Phys.* **1982**, *77,* 5593.
[50] J. Kolorenc, L. Mitas, *Rep. Prog. Phys.* **2011**, *74,* 026502.
[51] L. Spanu, S. Sorella, G. Galli, *Phys. Rev. Lett.* **2009**, *103,* 196401.
[52] R. Maezono, N. D. Drummond, A. Ma, R. J. Needs, *Phys. Rev. B* **2010**, *82,* 184108.
[53] F. Sterpone, L. Spanu, L. Ferraro, S. Sorella, L.Guidoni, *J. Chem. Theor. Comput.* **2008**, *4,* 1428.
[54] S. Sorella, M. Casula, D. Rocca, *J. Chem. Phys.* **2007**, *127,* 14105.
[55] F. Schautz, C. Filippi, *J. Chem. Phys.* **2004**, *120,* 10931.
[56] P. M. Zimmermann, J. Toulouse, Z. Zhang, C. B. Musgrave, C. J. Umrigar, *J. Chem. Phys.* **2009**, *131,* 124103.
[57] M. Caffarel, M. Rerat, C. Pouchan, *Phys. Rev. A* **1993**, *47,* 3704.
[58] E. Coccia, O. Chernomor, M. Barborini, S. Sorella, L. Guidoni, *J. Chem. Theory Comput.* **2012**, *8,* 1952.
[59] D. Bressanini, G. Morosi, M. Mella, *J. Chem. Phys.* **2002**, *116,* 5345.
[60] N. Metropolis, A. W. Rosenbluth, M. N. Rosenbluth, A. H. Teller, E. Teller, *J. Chem. Phys.* **1953**, *21,* 1087.
[61] C. J. Umrigar, *Int. J. Quantum Chem.* **1989**, *36,* 217.
[62] C. Filippi, C. J. Umrigar, *Phys. Rev. B* **2000**, *61,* 16291.
[63] R. Assaraf, M. Caffarel, *J. Chem. Phys.* **2003**, *119,* 10536.
[64] S. Sorella, L. Capriotti, *J. Chem. Phys.* **2010**, *133,* 234111.
[65] C. Attaccalite, S. Sorella, *Phys. Rev. Lett.* **2008**, *100,* 114501.
[66] L. Pauling, The nature of the Chemical Bond, 3rd ed.; Cornell University Press: Itaca, New York, **1960**.
[67] S. Sorella, Turborvb quantum monte carlo package, Available at: http://people.sissa.it/∼sorella/web/index.html (accessed date 11 may, 2012).
[68] M. Casula, S. Sorella, *J. Chem. Phys.* **2003**, *119,* 6500.
[69] M. Marchi, S. Azadi, S. Sorella, *Phys. Rev. Lett.* **2011**, *107,* 086807.
[70] T. D. Beaudet, M. Casula, J. Kim, S. Sorella, R. Martin, *J. Chem. Phys.* **2008**, *129,* 164711.
[71] M. Marchi, S. Azadi, M. Casula, S. Sorella, *J. Chem. Phys.* **2009**, *131,* 154116.
[72] N. D. Drummond, M. D. Towler, R. J. Needs, *J. Phys. Rev. B* **2004**, *70,* 234119.
[73] S. Sorella, *Phys. Rev. B* **2005**, *71,* 241103(R).
[74] C. J. Umrigar, J. Toulouse, C. Filippi, S. Sorella, R. G. Hennig, *Phys. Rev. Lett.* **2007**, *98,* 110201.
[75] F. R. Petruzielo, J. Toulouse, C. J. Umrigar, *J. Chem. Phys.* **2011**, *134,* 064104.
[76] M. Burkatzki, C. Filippi, M. Dolg, *J. Chem. Phys.* **2007**, *126,* 234105.
[77] M. Burkatzki, C. Filippi, M. Dolg, *J. Chem. Phys.* **2008**, *129,* 164115.
[78] C. Filippi and C. J. Umrigar, *J. Chem. Phys.* **1996**, *105,* 213.
[79] N. Nemec, M. D. Towler, R. J. Needs, *J. Chem Phys.* **2010**, *132,* 034111.
[80] D. C. Teller, T. Okada, C. A. Behnke, K. Palczewski, R. E. Stenkamp, *Biochemistry* **2001**, *40,* 7761.

Received: 14 May 2012
Revised: 22 June 2012
Accepted: 26 June 2012
Published online on 17 July 2012